Conformation-Specific Spectroscopy and Excited State Photophysics of 5-Phenyl-1-pentene

Nathan R. Pillsbury and Timothy S. Zwier*

Department of Chemistry, Purdue University, 560 Oval Drive, West Lafayette, Indiana 47907

Received: July 28, 2008; Revised Manuscript Received: October 7, 2008

Single-conformation spectroscopy of 5-phenyl-1-pentene has been studied in a supersonic expansion by using a combination of methods, including resonant two-photon ionization (R2PI), ultraviolet hole-burning (UVHB), and rotational band contour analysis. Five conformational isomers (labeled A−E) have been identified in the spectrum, with S_0-S_1 origins at 37518, 37512, 37526, 37577, and 37580 cm^{-1}, respectively. Rotational band contours of these origin transitions recorded at 0.08 cm^{-1} resolution reflect the sensitivity of the direction of the transition dipole moment (TDM) to the conformation of the pentene side chain. On the basis of a comparison of the observed rotational band contours with that predicted by M05-2X/6-31+G* and CIS/6-31G calculations, firm assignments have been obtained for four of the five conformers, while the fifth is constrained to one of two possibilities. On the basis of values of three torsional angles along the pentene chain [about the C(α)−C(β) (τ_1), C(β)−C(γ) (τ_2), and C(γ)−C(δ) (τ_3) bonds], the conformers can be uniquely labeled. By using this scheme, the assigned conformations are ggH_γ' for A, gaH_γ' for B, gaH_γ for C, agH_γ for D, and either aaH_γ or agH_γ' for E. Single vibronic level fluorescence lifetimes have been recorded for a series of vibronic levels in the range 0−1500 cm^{-1} for all five conformers. A sharp drop in lifetime of all five conformers at ∼1000 cm^{-1} is proposed to accompany overcoming a rate-limiting barrier to exciplex formation.

I. Introduction

Hydrocarbon fuels are complicated mixtures that contain a range of aromatic molecules, including alkylbenzenes. During the combustion process, these substituted benzenes play a significant role in the formation of larger polyaromatic hydrocarbon (PAH) molecules that eventually lead to the formation of soot.[1,2] Among the pathways to be considered are those that involve formation of one structural isomer of a molecule, followed by intramolecular isomerization to a fused ring product. In such cases, conformational isomerization may need to precede structural isomerization by bringing the reacting segments in close enough proximity for reaction to occur. Determining the conformational preferences and single-conformation spectroscopic signatures provides a necessary foundation for studies that seek to understand the effects of conformational complexity on combustion processes involving these types of molecules. The present paper describes such studies, focusing attention on 5-phenyl-1-pentene (5PPene). This specific choice is dictated in part by the intriguing photophysics and photochemistry of this molecule.

Possible exciplex formation of 5PPene was indirectly implicated in gas phase and solution photochemistry experiments at room temperature.[3−5] Morrison and co-workers surmised that a double bond, three carbons removed from a benzene ring, is efficient in trapping the S_1 state of the phenyl ring.[3−5] By forming an exciplex between the phenyl ring and the terminal vinylic double bond, the S_1 excited state of the phenyl ring is stabilized in configurations that bring the double bond over the phenyl ring. Exciplex formation in solution showed itself as a decrease in lifetime of the excited state from 35 ns in toluene (where exciplex formation is not possible) to 2.5 ns in 5PPene.[3,5] Exciplex formation was also consistent with the observed photocycloaddition products on both solution and gas phase.[4] Because the primary products involve meta cycloadducts of interest in many natural products, this photochemistry has been studied in some detail over the intervening years.[4]

In solution, the observed behavior is a weighted average of that due to all conformational isomers. Furthermore, the excited state reaction occurs in competition with vibrational relaxation to the solvent. In the gas phase, conformation-specific spectroscopy can identify the conformers present. Having done so, it is possible to study the UV spectra of these isomers to search for conformation-specific photophysics indicative of exciplex formation. Barriers to exciplex formation from different starting structures could be reflected in different lifetimes as a function of energy above the electronic origin.

Studies like the present one build on a rich foundation of past studies of the spectroscopy and dynamics of substituted benzenes. Earlier work by Smalley and co-workers on a range of substituted benzenes with increasingly long, flexible tails (alkylbenzenes, alkynylbenzenes, etc.) in a jet-cooled environment identified transitions due to multiple isomers, but did not make assignments to specific structures.[6] Instead, they used dispersed emission to study intramolecular vibrational energy redistribution (IVR) within the S_1 manifold as a function of the vibrational density of states.[7] They did, however, observe a small red-shift of *gauche* conformations with respect to *anti* conformations and attributed this to the interaction between a γ-hydrogen in the alkyl chain and the π-cloud of the phenyl ring in *gauche* structures.[6] Recently, several groups, including our own, have returned to some of these molecules to study their conformation-specific spectroscopy.[8−11] Studies by the groups of Simons and Pratt have been particularly helpful in identifying general features of the spectroscopy of these molecules.[8,9] In particular, they have found that there is a substantial change in the transition dipole moment (TDM) direction (∼30°) between *gauche* and *anti* structures. They ascribe this change in the TDM direction to the off-axis nature of the *gauche* structures causing the excited state molecular

* To whom correspondence should be addressed. E-mail: zwier@purdue.edu.

10.1021/jp806691w CCC: $40.75
Published on Web 12/09/2008

orbitals to mix, thereby forming $^1L_a/^1L_b$ states of mixed character.[9] This produces an extraordinary sensitivity of the shape of the rotational band contour to conformation and provides a powerful diagnostic of the conformation. Fortunately, CIS calculations correctly predict the change in TDM directions to within a few degrees of the experiment for the alkylbenzenes.[9] These features have been used recently by Selby et al. to make firm spectroscopic assignments for several other flexible substituted benzenes.[11]

The purpose of this paper is to spectroscopically characterize the low-energy conformational isomers of 5PPene. Such studies enable us to search for conformation-specific excited state dynamics. They also lay the groundwork for future studies that measure the barriers to conformational isomerization by using stimulated emission pumping-population transfer (SEP-PT) spectroscopy, a method developed in our laboratory specifically for this purpose.[10,12−16] Studies that characterize the potential energy surfaces of alkylbenzenes such as this can be used by those seeking to better model the intricate pathways that lead toward PAH formation.

II. Methods

A. Experimental Details. The apparatus and methods used in this study have been described previously.[10,11,17,18] Briefly, the present study used a combination of methods, including one-color resonant two-photon ionization (1C-R2PI) to record the excitation spectrum, ultraviolet hole-burning (UVHB) to acquire ultraviolet excitation spectra of single conformations, and 2C-R2PI to obtain rotational band contours (RBC's) and excited state lifetimes. All experiments were conducted by using the frequency doubled output of Nd:YAG pumped dye lasers (Coumarin 540A and Coumarin 503 laser dyes purchased from Exciton). Laser powers for the 1C-R2PI experiment were kept to ∼0.15 mJ/pulse at a repetition rate of 20 Hz. The probe laser in the UVHB experiment was also held near 0.15 mJ/pulse while the hole-burn (HB) laser power was five times higher (0.75 mJ/pulse) in order to at least partially saturate the transition of interest. The probe and HB lasers were separated in time by about 700 ns (to avoid two-color enhancement) with the HB laser firing first. Tuning the probe laser and monitoring the difference in ion signal (using active baseline subtraction from a gated integrator) between successive probe pulses (with and without the HB laser present) yielded the UVHB spectra.

An intracavity etalon was used to increase the resolution of the dye laser for rotational band contour scans (0.08 cm^{-1} in the ultraviolet). Scans were recorded by angle tuning the etalon under computer control. The resonant laser power was kept very low (∼20 μJ/pulse) to avoid saturation broadening. The ionization laser was sufficiently high (∼1.0 mJ/pulse) to maximize the efficiency of ionization of the excited state molecules.

Excited state lifetimes were recorded with the first laser (excitation laser) fixed on a particular vibronic transition in the R2PI spectrum and the second laser (ionization laser) fixed a nonresonant wavelength to the red of the origin band. The time between the laser pulses was scanned while recording the intensity of the two-color signal at each time interval. To determine the lifetimes, these plots were least-squares fit to a single exponential decay function.

An initial sample (∼500 mg) of 5PPene (with a purity of ∼99%) was obtained from the Morrison group at Purdue for preliminary studies. When this sample was exhausted, a synthesis was performed by following the procedure outlined by Ho et al.[4] involving a Grignard reaction with 1-bromo-2-phenylethane and allylmagnesium bromide as reactants. 5PPene was produced with about 60% yield. No further purification was attempted due to the fact that our experiment incorporates mass resolution. To create the free jet expansion, a total pressure of 1.4 bar of helium was passed through a sample reservoir inside a pulsed valve (R. M. Jordan Co.), which internally heats to about 70 °C. This gaseous mixture was then introduced into the vacuum chamber through a pulsed valve with 800 μm orifice at a repetition rate of 20 Hz.

TABLE 1: ZPE Corrected Relative Energies (kcal/mol) of the Calculated Conformational Minima of 5PPene

level of theory/ basis set	aaH_γ	agH_γ	gaH_γ'	gaH_γ	aaC_β	agH_γ'	ggH_γ'	gaC_β
B3LYP/6-31+G*	0.00	0.41	0.68	0.77	0.79	0.99	1.28	1.64
MP2/6-311++G**	1.47	1.18	0.84	0.85	2.23	−[a]	0.00	1.69
M05-2X/6-31+G*	0.37	0.27	0.42	0.45	0.83	1.17	0.00	0.55

[a] No minimum found.

B. Computational Methods. To acquire starting structures for the possible conformational isomers of 5PPene, molecular mechanics (MM) calculations were carried out using the MMFFs force field.[19,20] Once these structures were identified, full energy optimizations were carried out using density functional theory (DFT) with Becke3LYP[21,22] and M05-2X[23] functionals (6-31+G* basis set). The M05-2X functional was designed by Truhlar and co-workers to better account for dispersive interactions.[23] These structures were also subjected to second-order Møller−Plesset perturbation theory[24−29] (MP2) (6-311++G** basis set) for comparison with the DFT results. Configuration interaction singles[30] (CIS) (6-31G basis set) and Hartree−Fock (HF) calculations (6-31G basis set) were performed to obtain the ground and excited state rotational constants as well as the transition dipole moment (TDM) directions for use in simulating the rotational band contours.

MM calculations were completed with the Macromodel software package.[31] Gaussian03[32] was employed to carry out the DFT, MP2, CIS, and HF computations. The rotational band contour simulations used the JB95 rotational fitting program.[33,34]

III. Results and Analysis

A. Computational Predictions. The MMFFs force field identified 14 conformational isomers of 5PPene within the first 15 kJ/mol. The eight lowest energy structures were then optimized with DFT B3LYP/6-31+G*, and harmonic vibrational frequency calculations were carried out. MP2/6-311++G** optimizations were also performed to compare to the B3LYP results. Table 1 compares the zero-point corrected relative energies of the eight lowest energy conformers at the B3LYP and MP2 levels of theory. The B3LYP results predict the *anti/anti* (aa) structure to be the lowest in energy, while the MP2 results put the aa structure up at one of the highest of the eight predicted conformers. However, the structures optimized by the two methods are nearly identical, indicating that the basis set is not responsible for these energy differences. Instead, something inherent to the methods must be causing these differences in energy. It is well-known that DFT/B3LYP calculations do not properly account for dispersion forces, and that MP2 calculations overestimate them in certain circumstances, and also suffer from substantial basis set superposition error (BSSE) unless very large basis sets are employed.[35] This is the likely cause of the energy discrepancy observed between the two methods, since the MP2 calculations systematically lower the energies of structures in which part of the alkyl chain is in close proximity to the ring, where dispersive interactions should play a greater role.

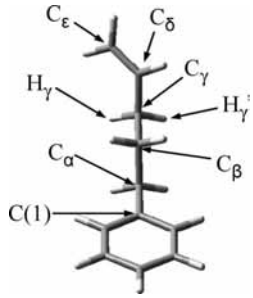

Figure 1. Example structure of 5-phenyl-1-pentene with relevant atoms labeled.

TABLE 2: Dihedral Angle Values from B3LYP Optimizations

	aaH_γ	agH_γ	gaH_γ'	gaH_γ	aaC_β	agH_γ'	ggH_γ'	gaC_β
$\tau_1°$	180	180	−65	−65	180	177	−67	−65
$\tau_2°$	−178	67	179	−176	180	64	−67	178
$\tau_3°$	−120	−122	118	−121	0	115	126	1

Several groups have recently sought to improve the way in which DFT methods account for dispersive interactions. Among the promising solutions is the M05-2X functional devised by Truhlar and co-workers.[36,37] On the basis of tests so far carried out, the M05-2X functional outperforms both B3LYP and MP2 in cases where hydrogen bonding and dispersion forces are important. The results of the M05-2X/6-31+G* optimizations of 5PPene are also included in Table 1. This DFT method seems to agree with MP2 in that they both predict the gg conformer to be the global minimum. However, they disagree on the energy ordering of the ga versus the ag and aa structures. MP2 finds the two *anti* structures to be lower in energy than the ga structures, while M05-2X predicts the opposite. The present experimental data can provide a test of these methods, following experimental determination of the conformational assignments.

Each calculated structure of 5PPene was uniquely named by describing the dihedral angles of the alkyl chain. An example structure is given in Figure 1. The carbon atoms of the chain are labeled starting from the carbon atom in the phenyl ring to which the chain is attached, called C(1). The five C atoms of the chain starting with the atom bound to C(1) are labeled C_α, C_β, C_γ, C_δ, and C_ϵ (illustrated in Figure 1). The dihedral angles of the alkyl chain are labeled as follows: $\tau_1 = C(1)-C_\alpha-C_\beta-C_\gamma$, $\tau_2 = C_\alpha-C_\beta-C_\gamma-C_\delta$, and $\tau_3 = C_\beta-C_\gamma-C_\delta-C_\epsilon$. Finally, the structures were given unique names that use the following criteria: $\tau_{1\text{ or }2} = \pm 180° \leftrightarrow$ a (*anti*), $\tau_{1\text{ or }2} = \pm 60° \leftrightarrow$ g (*gauche*), $\tau_3 = 0° \leftrightarrow C_\beta$ (eclipsed with C_β), $\tau_3 = -120° \leftrightarrow H_\gamma$ (eclipsed with H_γ), and $\tau_3 = 120° \leftrightarrow H_\gamma'$ (eclipsed with H_γ'). For example, the structure in Figure 1 is named aaH_γ because $\tau_1 \approx 180°$, $\tau_2 \approx 180°$, and $\tau_3 \approx -120°$. The names of all of the structures and the values of their respective dihedral angles are given in Table 2. We must, however, recognize that since no chiral center exists in this molecule, a spectroscopically indistinguishable mirror image ($-\tau_1$, $-\tau_2$, $-\tau_3$) exists for each of the different conformational isomers and that a complete naming scheme should include the direction of rotation for gauche dihedrals (e.g., g_+, g_-). However the current scheme will suffice for the treatment of the spectroscopy.

B. 1C-R2PI and UVHB Spectra. The 1C-R2PI and UVHB spectra of 5PPene are shown in Figure 2. These spectra are very similar to those obtained by Smalley and co-workers in their study of alkylbenzenes, although no hole-burning was carried out in that work.[6] This is not surprising since most of the Franck-Condon activity is in the in-plane ring modes typical of the

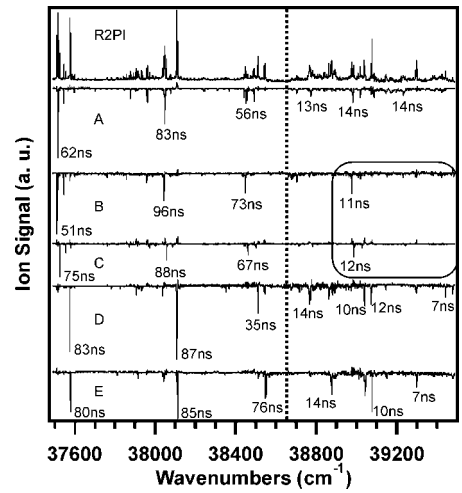

Figure 2. 1C-R2PI and UVHB spectra of conformers A−E over the 37 500−39 500 cm^{-1} region. The number labels on selected transitions are the S_1 lifetimes of the respective bands. The circled area of the spectra of conformers B and C highlights the intensity cutoff observed in these spectra.

TABLE 3: Experimental Frequencies of the S_1 Benzene-Like Ring Modes of 5PPene

	freq (cm^{-1})					
conformer	0^0_0	$6a^1_0$[a]	$6b^1_0$[a]	1^1_0[a]	12^1_0[a]	18^1_0[a]
A	0.0 (37518)	441.9	529.6		935.1	972.8
B	0.0 (37512)	444.5	530.2		934.2	
C	0.0 (37526)	444.6	529.8		933.8	972.7
D	0.0 (37577)	458.8	530.5	772.7	933.4	966.8
E	0.0 (37580)	463.2	530.6	767.3	932.3	968.4

[a] Assignments were made by comparison to frequencies observed for *n*-pentylbenzene[6] and 5-phenyl-1-pentyne.[11]

S_0-S_1 transitions in alkylbenzenes: 6a, 6b, 12, 18 (using Versanyi rules for describing modes of substituted benzenes).[38] Five conformations were observed in the free jet expansion, labeled A−E, with origin transitions at 37 518, 37 512, 37 526, 37 577, and 37 580 cm^{-1}, respectively. Band assignments for the S_1 ring modes were made by comparing the experimental frequencies with those seen previously by Selby and Zwier in its close analogue 5-phenyl-1-pentyne (5PPyne)[11] and by Smalley et al. for *n*-pentylbenzene.[6] The S_1 ring mode experimental frequencies and band assignments of 5PPene are given in Table 3. As mentioned in the Introduction, on the basis of previous work,[6,8,9,11] it is typically the case that *gauche* structures have red-shifted origin transitions, based on the preferential stabilization of the S_1 state provided by the interaction of the γ-methylene hydrogen(s) with the π-cloud of the phenyl ring.[6] In addition, conformers A−C all possess Franck−Condon activity in low-frequency torsional vibrations that is not present in the spectra of conformers D and E, consistent with a stronger interaction of the *gauche* structures with the phenyl ring. Thus, we tentatively assign the A−C origin transitions which are shifted to the red as *gauche* ($\tau_1 = -60°$) structures, and the two to the blue (D and E) as *anti* ($\tau_1 = 180°$) structures.

C. Rotational Band Contours. Rotational band contours of conformers A−E were recorded and fit by using the rotational fitting program JB95. The spectra of conformers A−C are shown in Figure 3a−c, while those for conformers D and E are shown in Figure 4a,b. The top traces are the experimental spectra and the bottom traces are the corresponding "best fits". The fitting procedure is similar to that carried out by Selby and Zwier[11] and by Dickinson et al.[39] Preliminary contours were generated

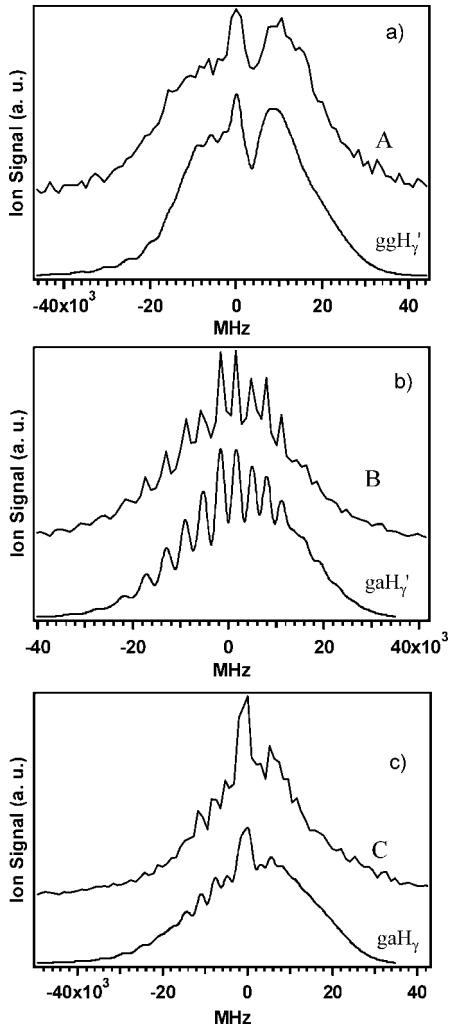

Figure 3. (a−c) The experimental RBC (top) and "best fit" contours (bottom) of conformers A−C, respectively.

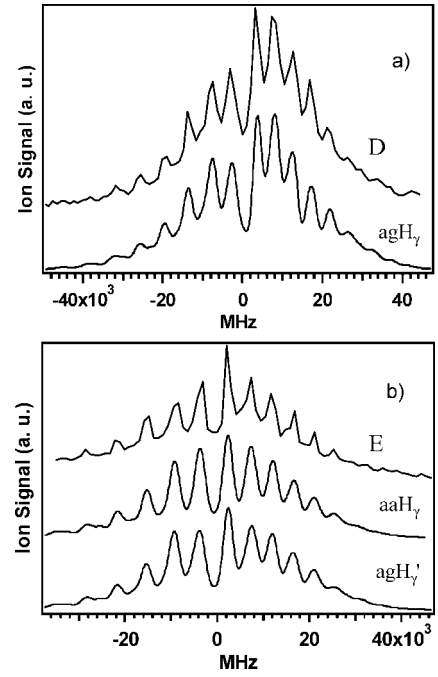

Figure 4. (a,b) The experimental RBC (top) and "best fit" contours (bottom) of conformers E and D, respectively. Since conformer E could not be assigned to a single structure, both possible fits are shown.

by using ground state rotational constants predicted by DFT M05-2X/6-31+G* calculations. Initial values for the changes in rotational constants with electronic excitation were taken from a comparison of the CIS excited state results with HF calculations, using the same basis set. TDM directions were taken from the CIS calculations. These simulations were then visually compared to the experimental contours to make preliminary assignments. Next, the temperature and resolution were adjusted to better match the experimental traces. Finally, the main fit parameters were adjusted to get the best fit possible. First, where the resolution allowed, the experimental values of $(A - B_{ave})'$ and $(A - B_{ave})''$ (where $B_{ave} = {}^1/_2(B + C)$) were calculated from the ^{P}Q and ^{r}Q sub-band head spacings. Then A' and A'' were varied to match the experimental $(A - B_{ave})'$ and $(A - B_{ave})''$ values, while all other parameters were kept at their calculated values. Next, B' and C' were adjusted slightly to improve the fit quality, while maintaining B'' and C'' at their calculated values. Finally, the TDM direction was adjusted to account for any intensity discrepancies. The calculated input parameters for the contour fits and the best fit output values from JB95 are shown in Table 4.

1. Assignments of Gauche Conformers. *Conformer A.* The contour of conformer A is shown in Figure 3a. The sharp Q-branch in the experimental contour is indicative of significant "a" character to the TDM for this conformer. According to the calculations, only the ggH$_\gamma'$ and gaC structures have their TDM's mostly along the "a" rotational axis. After obtaining best fits for both structures it was clear that the ggH$_\gamma'$ fit stood out as the closest match. The simulated contour of the gaC isomer showed too large of a spacing between the Q- and R-branches (>10 MHz) and was slightly broader in width. Therefore, we assign conformer A to the ggH$_\gamma'$ structure whose best fit contour is presented at the bottom of Figure 3a.

Conformer B. The rotational contour of the S_0-S_1 origin of conformer B is shown in Figure 3b. This band is readily assigned since only the gaH$_\gamma'$ conformer produced a fit that was relatively close to the experiment. Therefore, we assign conformer B to the gaH$_\gamma'$ structure. It is worth noting that, of the five observed conformers, the CIS calculation showed the largest discrepancy with experiment for this structure (gaH$_\gamma'$), predicting a TDM direction of 27:23:50 (% a:% b:% c) compared to the best fit TDM direction of 4:14:82. It also is the structure with the largest discrepancy between calculated and experimental values for the *A* rotational constant. The gaH$_\gamma'$ structure has the pentene chain nearly perpendicular to the ring, with significant ring-chain interaction via the C$_\gamma$ hydrogen(s). It seems likely that both the *A* rotational constant and the TDM direction may be particularly sensitive to the strength and position of the $C_\gamma H_2-\pi$ interaction, which may not be properly accounted for in CIS calculations.

Conformer C. Like "B", a unique assignment for conformer C followed readily from the predicted contours, since only the gaH$_\gamma$ structure gave a close match to the experimental contour (Figure 3c, top). In this case, the best fit values for the rotational constants and TDM were very close to the starting values from the CIS calculations. On this basis, we assign conformer C to the gaH$_\gamma$ structure (Figure 3c bottom). This structure differs from that of conformer B in the orientation of the vinyl group relative to the alkyl chain, which is eclipsed with the C$_\gamma$ hydrogen that interacts most strongly with the phenyl ring. This lowers the *A* rotational constant significantly relative to that in conformer C.

2. Assignments of Anti Conformers. *Conformer D.* The rotational band contour of conformer D (shown at the top of Figure 4a) is a B-type rotational band contour, with nearly

TABLE 4: Calculated Input Parameters and Experimental Best Fit Output Values from the Rotational Contour Analysis

	calculations					
parameter	ggH_γ'	gaH_γ'	gaH_γ	agH_γ	aaH_γ	agH_γ'
A'' (MHz)[a]	1922	2281	1926	3121	3190	3245
B'' (MHz)[a]	720	520	575	463	413	451
C'' (MHz)[a]	596	500	538	434	396	415
$(A - B_{avg})''$ (cm^{-1})[a]	0.0421	0.0590	0.0457	0.0891	0.0929	0.0937
ΔA (MHz)[b]	−48	−78	−53	−83	−124	−95
ΔB (MHz)[b]	0	−1	−1	−2	−1	−2
ΔC (MHz)[b]	−1	0	0	−3	−2	−3
% a:% b:% c[c]	53:33:14	27:23:50	16:2:82	3:94:3	0:98:2	4:96:0

	experimental fit					
parameter	A	B	C	D	E	
A'' (MHz)[e]	2019(8)	2284(7)	1967(5)	3169(9)	3219(8)	3243(7)
B'' (MHz)[d]	720	520	575	463	413	451
C'' (MHz)[d]	596	500	538	434	396	415
$(A - B_{avg})''$ (cm^{-1})[e]	0.0454(2)	0.0591(2)	0.0470(2)	0.0907(4)	0.0938(4)	0.0937(4)
ΔA (MHz)[e]	−121(7)	−86(6)	−42(5)	−143(7)	−138(10)	−147(9)
ΔB (MHz)[e]	−3(3)	−5(4)	4(2)	−2(4)	−4(3)	−17(3)
ΔC (MHz)[e]	21(4)	3(3)	10(3)	−3(4)	1(3)	3(2)
% a:% b:% c[f]	54:14:32	4:14:82	13:0:87	0:100:0	0:100:0	0:100:0
T (K)[e]	2.0(2)	1.5(1)	1.6(2)	1.7(1)	1.7(1)	1.7(2)
fwhm (cm^{-1})[e]	0.08(1)	0.07(1)	0.08(1)	0.07(1)	0.08(1)	0.08(1)

[a] Predicted from the M05-2X/6-31+G* level of theory. [b] Predicted from HF/6-31G and CIS/6-31G levels of theory. [c] Predicted from the CIS/6-31G level of theory. [d] Held at calculated values. [e] Estimated experimental error shown in parentheses as the error associated with the last significant digit. [f] Estimated error in the TDM is ∼5%.

equally spaced band heads due to the molecule being a near-prolate symmetric rotor in which $B' \approx B''$ and $A' \approx A''$. This results in a rotational band structure that is dominated by ^pQ and ^rQ sub-bands with a spacing between adjacent band heads of $2(A' - B')$.[40] For conformer D, this spacing is ∼0.17 cm^{-1}, indicating an A′ rotational constant of ∼0.10 cm^{-1} (∼3000 MHz). In this case, three of the conformations (agH_γ, aaH_γ, and agH_γ'), all of which are *anti* about the $C_\alpha - C_\beta$ bond, are predicted to have nearly pure B-type contours with A′ rotational constants in this range. Best fit contours were generated for each structure and ultimately led to a firm assignment. The results of both the aaH_γ and agH_γ' best fits showed A'' values very close to that of the calculated A'' values for agH_γ. Furthermore, the agH_γ best fit contour resulted in parameters which closely resembled the calculated rotational constants and TDM for the agH_γ structure. Therefore, conformer D has been assigned to the agH_γ structure, with its best fit contour shown at the bottom of Figure 4a.

Conformer E. Conformer E also has a B-type rotational band contour (Figure 4b, top) with nearly equally spaced band heads. The spacing between the bands is slightly larger than that of conformer D (∼0.18 cm^{-1}) making the A' rotational constant slightly greater than 3000 MHz. The two remaining anti structures (aaH_γ and agH_γ') both have A' rotational constants above 3000 MHz and TDM directions mostly along the *b*-rotational axis. Therefore, at the present experimental resolution, the best fits were nearly identical (Figure 4b, middle and bottom), preventing us from distinguishing with certainty which structure to assign to conformer E.

The assignments based on rotational band contours confirm our starting assumption based on the electronic frequencies of the $S_0 - S_1$ origins that A, B, and C were *gauche* structures in the τ_1 dihedral, while D and E were *anti* structures. Figure 5 presents a close-up view of the origin region of 5PPene with the assigned structures next to their respective $S_0 - S_1$ origins. Since the rotational analysis did not yield a firm assignment for "E", both possible structures are shown. We will return to consider the relative merits of both assignments in the Discussion section.

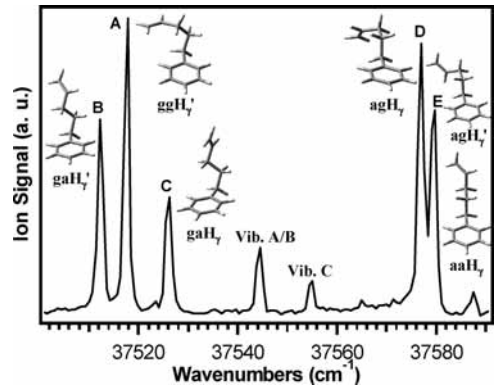

Figure 5. Expanded region of the origin transitions in the 1C-R2PI of 5PPene with their corresponding assigned structures. Both possible structures of conformer E are shown.

D. Excited State Dynamics. Armed with knowledge of the UVHB spectra of each of the five observed conformers of 5PPene, we recorded single vibronic level (SVL) S_1 lifetimes for each of the five conformational isomers as a function of energy above the S_1 origin (Figure 2). Our goal was to determine whether conformation-specific differences in the SVL lifetimes might reflect differences in the energy barriers to exciplex formation. On the basis of these data, we can make several deductions immediately. First, the conformation-specific lifetimes of the vibronic bands become progressively shorter in vibronic levels more than 500 cm^{-1} above the S_1 origin (Figure 2). This is not unexpected, since previous studies of the alkylbenzenes,[41] 4-phenyl-1-butyne, and 5-phenyl-1-pentyne[11] also show a general decrease in the S_1 lifetime with increasing energy due to energy-dependent internal conversion or intersystem crossing. Second, unlike the other examples, in all of the conformations of 5PPene, the lifetimes of the vibronic bands drop off abruptly about 1000 cm^{-1} above the origin to values near 10 ns or shorter. Third, the lifetimes of the $S_0 - S_1$ origins

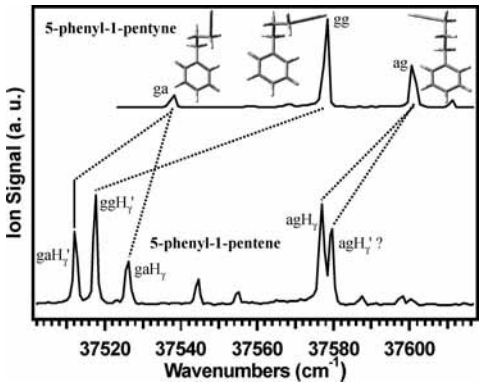

Figure 6. Comparison of the origin regions of 5PPyne (top) and 5PPene (bottom). The dotted lines highlight the similar structures of the two molecules. The question mark next to the agH$_\gamma'$ label indicates that it is a tentative assignment.

of the three *gauche* conformers A−C are shorter than those of their corresponding $6b^1_0$ bands. However, this is not the case for conformers D and E. Finally, as the UVHB spectra in Figure 2 show, the vibronic activity of conformers B and C cuts off above 1500 cm^{-1} (see the encircled region) while the other three conformers show relatively strong transitions all the way up to 2000 cm^{-1}. This could reflect a further reduction in S_1 lifetime peculiar to these conformers. We will address possible explanations for these observations in the Discussion section.

IV. Discussion and Conclusions

A. The Conformational Preferences of 5-Phenyl-1-pentene. We have recorded single conformation ultraviolet spectra of 5-phenyl-1-pentene and determined that five conformational isomers exist in the supersonic expansion. Firm assignments have been made for four of the five isomers by recording and simulating the rotational band contour of each S_0-S_1 origin band, while the fifth (conformer E) has been constrained to one of two *anti* structures (aaH$_\gamma$ and agH$_\gamma'$). Conformers A−C are all *gauche* structures about the $C_\alpha-C_\beta$ bond, with A assigned to ggH$_\gamma'$, B to gaH$_\gamma'$, and C to gaH$_\gamma$. Conformer D has been assigned to the agH$_\gamma$ structure.

Given the close structural similarity between 5PPene and 5-phenyl-1-pentyne (5PPyne), the subject of a recent single-conformation spectroscopy investigation,[11] it is worth comparing the conformation-specific spectra and assignments in the two molecules. Since 5PPene has an extra degree of freedom in the hindered rotation of the vinyl group, we expected to observe more conformations in 5PPene than were seen for 5PPyne. Indeed, only three conformers of 5PPyne were observed in the jet, assigned to ag, gg, and ga structures.[11] The aa conformer was not detected in that study, despite being calculated as a low-lying minimum by DFT methods (Table 1). Close-up views of the S_0-S_1 origin regions of 5PPene and 5PPyne are compared in Figure 6. The dotted lines are included to highlight the shifts and splittings of the different conformers of 5PPene relative to 5PPyne. As in 5PPyne, the shift between the ag and ga conformers of 5PPene is about 60 cm^{-1}. As previously explained, the *gauche* structures have one of the γ-hydrogens out over the benzene ring, producing the observed red-shift. An additional source of S_1 state stabilization appears to be in play in the gg conformer of 5PPene, which must arise from the vinyl group interaction with the phenyl ring, which is at the right orientation and a closer distance than in the other conformers.

The comparison of these two spectra also clearly shows the consequences of having a terminal vinyl group rather than an ethynyl group. The vinyl group has two possible configurations while the ethynyl group only has one. Therefore, in cases where the same conformations are observed in both molecules, the single peak in 5PPyne should be split into two transitions due to the H$_\gamma$/H$_\gamma'$ pair. This is indeed the case for the ga conformer of 5PPyne (Figure 6), whose single transition shifts and splits into two separate transitions in 5PPene (gaH$_\gamma$ and gaH$_\gamma'$). On the other hand, conformer A of 5PPene (ggH$_\gamma'$) does not have a transition assignable to its ggH$_\gamma$ counterpart, most likely because of steric constraints between the pentene chain and the ortho-hydrogen atom on the benzene ring, which raises the energy of this conformation (Table 1). Finally, as the dotted lines connecting the ag conformer of 5PPyne to the pair of *anti* transitions of 5PPene suggests, a tentative assignment of conformer E to agH$_\gamma'$ rather than aaH$_\gamma$ is made plausible by the comparison to 5PPyne, thereby completing the H$_\gamma$/H$_\gamma'$ pair, could be made. However, the results of the calculations (Table 1) clearly favor the aaH$_\gamma$ isomer, which is almost 1 kcal/mol more stable than agH$_\gamma'$ at the DFT B3LYP and M05-2X calculations, while the MP2 calculation for agH$_\gamma'$ shows no stable minimum for this structure. To resolve the assignment of conformer E with certainty, higher resolution UV spectra would be helpful.

Finally, the firm assignments for conformers A−D can provide a check on the accuracy of the calculations as a function of the level of theory. In the limit that the oscillator strengths or Franck−Condon factors do not vary significantly from one conformer to the next, the relative intensities of the S_0-S_1 origin transitions reflect the relative populations of the conformers. The most intense transition in the spectrum is transition A (Figure 5), assigned to ggH$_\gamma'$. This conformer is calculated to be the global minimum according to both MP2 and M05-2X calculations, while B3LYP predicts it to be among the highest energy conformers (seventh out of the eight in Table 1). This highlights a well-known deficiency of B3LYP calculations, already mentioned, involving a systematic underestimation of dispersive attractions.[36,42−44] The next most intense transitions are those assigned to the *anti* pair of conformers D and E. The MP2 calculations do not reflect this trend, but instead push the agH$_\gamma'$, aaH$_\gamma$, and agH$_\gamma'$ conformers up in energy to the point that the former two are among the highest energy conformers, while the latter is not even a stable minimum on the surface. The likely reason for this inconsistency is the systematic overstabilization of structures that maximize interaction of the chain with the ring (e.g., *gauche* versus *anti*) via MP2 methods. van Mourik and co-workers have recently explored the reasons for this overstabilization, ascribing it to a combination of two effects: (i) intramolecular basis set superposition error (BSSE),[35] which plagues standard MP2 calculations with all but the largest basis sets (e.g., aug-cc-PVTZ or higher[45−50]), and (ii) a systematic over-estimation of dispersive interactions. Knowledge of these complementary discrepancies of B3LYP and MP2 calculations motivated our inclusion of calculations that use Truhlar's recently developed M05-2X functional in DFT calculations, a functional designed explicitly to more accurately account for dispersive effects within the DFT framework.[23] The DFT M05-2X calculations predict a relative energy ordering [E(A) < E(D) < E(B) ~ E(C)] in keeping with the relative intensities of the A−D origins. If one were to rely on the energy ordering of the M05-2X calculations in distinguishing between the two possible assignments for conformer E, it would lead to a clear preference for the assignment of this conformer as aaH$_\gamma$ rather than agH$_\gamma'$.

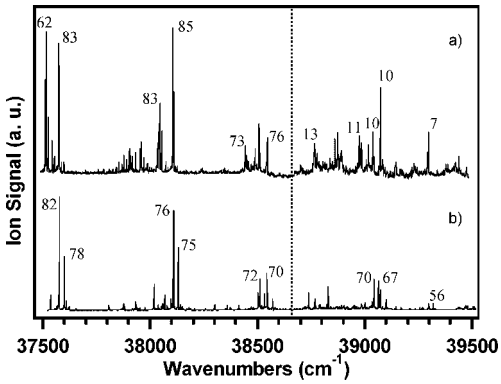

Figure 7. 1C-R2PI spectra of (a) 5PPene and (b) 5PPyne with selected vibronic levels labeled with their respective S_1 lifetimes in nsec. The vertical dotted line indicates the point at which the vibronic lifetimes of 5PPene drop suddenly.

B. Conformation-Specific Photophysics. One of the motivations of the present study was providing a conformation-specific view of the photophysics (and potentially photochemistry) of 5PPene. To that end, we measured SVL S_1 lifetimes for each of the five conformers as a function of energy above the S_1 origins, the results for which have already been described in Section III.D. There we identified three aspects of the results that needed further consideration: (i) the sharp drop-off in S_1 lifetimes for all conformers above ~1000 cm^{-1} excess energy, (ii) the unusual lengthening of the S_1 lifetimes of the *gauche* conformers A−C between the S_1 origin and S_1 $6b^1_0$ transitions, and (iii) the apparent conformation-specific cutoff in the vibronic structure of conformers B and C at ~1500 cm^{-1} (Figure 2).

In seeking to understand these trends, we have compared our SVL lifetimes for 5PPene with the corresponding measurements on its close analogue 5-phenyl-1-pentyne (5PPyne), which we have recently studied.[11] A visualization of this comparison is given in Figure 7, where the SVL lifetimes for the two molecules are superimposed on the 1C-R2PI spectra of the two molecules. As the dotted line highlights, the sudden drop in the S_1 SVL lifetimes at an excess energy of ~1000−1200 cm^{-1} in 5PPene (Figure 7a) does not carry over to 5PPyne (Figure 7b), which shows long lifetimes out to ~2000 cm^{-1} excess energy. Therefore, we associate the presence of the terminal vinyl group with this sudden drop-off in lifetime, consistent with the notion that exciplex formation between the aromatic ring and vinyl group could be responsible for the reduced lifetimes. If exciplex formation is responsible for this sharp lifetime decrease, then the present results place bounds on the magnitude of the barrier to exciplex formation in the S_1 state at 1000−1200 cm^{-1}. The present data do not provide a direct measure of this energy barrier. However, we will report in the following article[51] on the results of an SEP-population transfer study of the conformational isomerization of 5PPene, which provides direct experimental bounds on the barriers to conformational isomerization between the five observed conformers A−E in the ground electronic state. Since these energy barriers reflect hindered rotation about the alkenyl chain C−C bonds, it seems likely that the experimental barriers obtained in S_0 will carry over to S_1 to some degree. One of the major findings of that study was that conformer A is separated from the other four conformers by energy barrier(s) somewhere in the 1200−1370 cm^{-1} region. While this is not a direct measure of the barrier to exciplex formation, it would be consistent with the experimental drop-off in lifetime if energies of this magnitude allowed access to regions of the potential energy surface that could lead to exciplex formation.

A similar line of argument also provides a tentative explanation for the unusual lengthening of the S_1 lifetime of the $6b^1$ levels of the *gauche* conformers A−C. The SEP-PT study[51] determined that conformers B and C, which differ only in the orientation of the vinyl group, are separated from one another in the ground state by a barrier below (but probably near in energy to) 621 cm^{-1}, which is well below all other barriers in the molecule. Thus, at the $6b^1$ level in S_1, it is plausible that conformers B and C can interconvert, so that the S_1 lifetime reflects some average of the two. Conformer A (ggH_γ') has an unobserved second conformer (ggH_γ) with a calculated relative energy 380 cm^{-1} above that of A, and a predicted barrier separating it from A of 880 cm^{-1}. In conformers D and E, where the same effect is not observed, the vinyl group is far from the ring, and therefore unaffected by this interconversion. We postulate, then, that these H_γ/H_γ' interconversions that reorient the vinyl group are responsible for the lengthening of the lifetime, though without further input from theory, the reason that this leads to a lengthening of the S_1 lifetime is not clear.

Finally we hypothesize that a higher energy barrier in the 1500 cm^{-1} region could be responsible for the conformation-specific cutoff in the spectrum of conformers B and C, which share the "ga" pentene backbone structure. These conformers (Figure 5) hold the pentene chain up over the ring and nearly perpendicular to it, seemingly poised to flop over by hindered rotation about the $C_\beta-C_\gamma$ bond to an exciplex structure. It is possible that a 1500 cm^{-1} barrier directly accesses an optimal exciplex structure, producing the cutoff in the 1C-R2PI spectra in this conformation-specific way. The proposed explanations for the observed conformation-specific lifetime behavior point out the need for further experimental and theoretical exploration of the excited state potential energy surface of 5PPene.

We end this discussion by returning to the solution-phase and room temperature gas phase studies of the photophysics and photochemistry of 5PPene to see what new insight the present studies can bring. In those studies, Morrison and coworkers established that, in solution, an olefin three carbons removed from a benzene ring readily traps the phenyl S_1 excited state to form an exciplex.[3,5] They surmised this after observing a reduction in the phenyl S_1 lifetime from 35 ns for toluene to 2.5 ns in 5PPene following excitation at 254 nm. In room temperature solution, 5PPene should relax to a Boltzmann distribution in the S_1 state on a time scale fast compared to fluorescence. The average internal energy of 5PPene at room temperature is 1700 cm^{-1}. If the barriers to isomerization are readily overcome at this internal energy, exciplex formation can occur, leading to the observed lifetime reduction. We have pinned down the threshold for this lifetime reduction to an energy region of about 1000−1200 cm^{-1}, consistent with the observation that interconversion to the exciplex is quite efficient at room temperature. At the same time, in solution, formation of *meta* cycloaddition photochemical products is strongly preferred over other possible cycloaddition products, occurring with a quantum yield of about 0.1.[4]

In the gas phase, the choice of photoexcitation wavelength can be used to tune the initial internal energy of the 5PPene molecules, with the time scale for thermalization dictated by the quencher pressure. The recent study by Ho and Morrison of the gas phase photochemistry of 5PPene detected a wider range of photoproducts when quenching was reduced, but all of the products were nevertheless consistent with formation of a vinyl/phenyl ring exciplex as an intermediate.[4] Future studies are needed that combine conformation-specific excitation with detection of specific products following collisional cooling,

thereby providing a more complete accounting of the pathways from unreactive conformer wells to exciplex and on to products.

Acknowledgment. This work was supported by the Department of Energy Basic Energy Sciences, Division of Chemical Sciences under Grant No. DE-FG02-96ER14656. N.R.P. acknowledges Purdue University and the Andrews family for the Frederick N. Andrews Fellowship. The authors also acknowledge David F. Plusquellic for his help with the JB95 rotational fitting program and Talitha M. Selby for her helpful discussions and early contributions to the 1C-R2PI and UVHB spectra.

References and Notes

(1) Tancell, P. J.; Rhead, M. M.; Pemberton, R. D.; Braven, J. *Fuel* **1996**, *75*, 717.
(2) Roubaud, A.; Lemaire, O.; Minetti, R.; Sochet, L. R. *Combust. Flame* **2000**, *123*, 561.
(3) Ferree, W.; Grutzner, J. B.; Morrison, H. *J. Am. Chem. Soc.* **1971**, *93*, 5502.
(4) Ho, C. D. D.; Morrison, H. *J. Am. Chem. Soc.* **2005**, *127*, 2114, and references cited therein.
(5) Morrison, H.; Ferree, W. I. *J. Chem. Soc. D* **1969**, 268.
(6) Hopkins, J. B.; Powers, D. E.; Smalley, R. E. *J. Chem. Phys.* **1980**, *72*, 5039.
(7) Hopkins, J. B.; Powers, D. E.; Mukamel, S.; Smalley, R. E. *J. Chem. Phys.* **1980**, *72*, 5049.
(8) Borst, D. R.; Joireman, P. W.; Pratt, D. W.; Robertson, E. G.; Simons, J. P. *J. Chem. Phys.* **2002**, *116*, 7057.
(9) Kroemer, R. T.; Liedl, K. R.; Dickinson, J. A.; Robertson, E. G.; Simons, J. P.; Borst, D. R.; Pratt, D. W. *J. Am. Chem. Soc.* **1998**, *120*, 12573.
(10) Selby, T. M.; Clarkson, J. R.; Mitchell, D.; Fitzpatrick, J. A. J.; Lee, H. D.; Pratt, D. W.; Zwier, T. S. *J. Phys. Chem. A* **2005**, *109*, 4484.
(11) Selby, T. M.; Zwier, T. S. *J. Phys. Chem. A* **2005**, *109*, 8487.
(12) Clarkson, J. R.; Baquero, E.; Zwier, T. S. *J. Chem. Phys.* **2005**, *122* (21), 214312.
(13) Clarkson, J. R.; Dian, B. C.; Moriggi, L.; DeFusco, A.; McCarthy, V.; Jordan, K. D.; Zwier, T. S. *J. Chem. Phys.* **2005**, *122* (21), 214311.
(14) Dian, B. C.; Clarkson, J. R.; Zwier, T. S. *Science* **2004**, *303*, 1169.
(15) Selby, T. M.; Zwier, T. S. *J. Phys. Chem. A* **2007**, *111*, 3710.
(16) Zwier, T. S. *J. Phys. Chem. A* **2006**, *110*, 4133.
(17) Arrington, C. A.; Ramos, C.; Robinson, A. D.; Zwier, T. S. *J. Phys. Chem. A* **1998**, *102*, 3315.
(18) Stearns, J. A.; Zwier, T. S. *J. Phys. Chem. A* **2003**, *107*, 10717.
(19) Halgren, T. A. *J. Comput. Chem.* **1996**, *17*, 490.
(20) Halgren, T. A.; Nachbar, R. B. *J. Comput. Chem.* **1996**, *17*, 587.
(21) Becke, A. D. *Phys. Rev. A* **1988**, *38*, 3098.
(22) Lee, C. T.; Yang, W. T.; Parr, R. G. *Phys. Rev. B* **1988**, *37*, 785.
(23) Zhao, Y.; Schultz, N. E.; Truhlar, D. G. *J. Chem. Theory Comput.* **2006**, *2*, 364.
(24) Frisch, M. J.; Head-Gordon, M.; Pople, J. A. *Chem. Phys. Lett.* **1990**, *166*, 275.
(25) Frisch, M. J.; Head-Gordon, M.; Pople, J. A. *Chem. Phys. Lett.* **1990**, *166*, 281.
(26) Head-Gordon, M.; Head-Gordon, T. *Chem. Phys. Lett.* **1994**, *220*, 122.
(27) Head-Gordon, M.; Pople, J. A.; Frisch, M. J. *Chem. Phys. Lett.* **1988**, *153*, 503.
(28) Møller, C.; Plesset, M. S. *Phys. Rev.* **1934**, *46*, 618.
(29) Saebo, S.; Almlof, J. *Chem. Phys. Lett.* **1989**, *154*, 83.
(30) Foresman, J. B.; Headgordon, M.; Pople, J. A.; Frisch, M. J. *J. Phys. Chem.* **1992**, *96*, 135.
(31) Mohamadi, F.; Richards, N. G. J.; Guida, W. C.; Liskamp, R.; Lipton, M.; Caufield, C.; Chang, G.; Hendrickson, T.; Still, W. C. *J. Comput. Chem.* **1990**, *11*, 440.
(32) Frisch, M. J.; Trucks, G. W.; Schlegel, H. B.; Scuseria, G. E.; Robb, M. A.; Cheeseman, J. R.; Montgomery, J. A., Jr.; Vreven, T.; Kudin, K. N.; Burant, J. C.; Millam, J. M.; Iyengar, S. S.; Tomasi, J.; Barone, V.; Mennucci, B.; Cossi, M.; Scalmani, G.; Rega, N.; Petersson, G. A.; Nakatsuji, H.; Hada, M.; Ehara, M.; Toyota, K.; Fukuda, R.; Hasegawa, J.; Ishida, M.; Nakajima, T.; Honda, Y.; Kitao, O.; Nakai, H.; Klene, M.; Li, X.; Knox, J. E.; Hratchian, H. P.; Cross, J. B.; Bakken, V.; Adamo, C.; Jaramillo, J.; Gomperts, R.; Stratmann, R. E.; Yazyev, O.; Austin, A. J.; Cammi, R.; Pomelli, C.; Ochterski, J. W.; Ayala, P. Y.; Morokuma, K.; Voth, G. A.; Salvador, P.; Dannenberg, J. J.; Zakrzewski, V. G.; Dapprich, S.; Daniels, A. D.; Strain, M. C.; Farkas, O.; Malick, D. K.; Rabuck, A. D.; Raghavachari, K.; Foresman, J. B.; Ortiz, J. V.; Cui, Q.; Baboul, A. G.; Clifford, S.; Cioslowski, J.; Stefanov, B. B.; Liu, G.; Liashenko, A.; Piskorz, P.; Komaromi, I.; Martin, R. L.; Fox, D. J.; Keith, T.; Al-Laham, M. A.; Peng, C. Y.; Nanayakkara, A.; Challacombe, M.; Gill, P. M. W.; Johnson, B.; Chen, W.; Wong, M. W.; Gonzalez, C.; Pople, J. A. *Gaussian 03*, Revision E.01; Gaussian, Inc.: Wallingford, CT, 2004.
(33) Meerts, W. L.; Schmitt, M.; Groenenboom, G. C. *Can. J. Chem.* **2004**, *82*, 804.
(34) Plusquellic, D. F.; Suenram, R. D.; Mate, B.; Jensen, J. O.; Samuels, A. C. *J. Chem. Phys.* **2001**, *115*, 3057.
(35) Shields, A. E.; van Mourik, T. *J. Phys. Chem. A* **2007**, *111*, 13272.
(36) Zhao, Y.; Truhlar, D. G. *J. Chem. Theory Comput.* **2007**, *3*, 289.
(37) Zhao, Y.; Truhlar, D. G. *Acc. Chem. Res.* **2008**, *41*, 157.
(38) Versanyi, G. *Vibrational Spectra of Benzene Derivatives*; Academic Press: New York, 1969.
(39) Dickinson, J. A.; Joireman, P. W.; Kroemer, R. T.; Robertson, E. G.; Simons, J. P. *J. Chem. Soc., Faraday Trans.* **1997**, *93*, 1467.
(40) Hollas, M. J. *High Resolution Spectroscopy*; John Wiley & Sons: West Sussex, England, 1998.
(41) Hopkins, J. B.; Powers, D. E.; Smalley, R. E. *J. Chem. Phys.* **1980**, *73*, 683.
(42) Perezjorda, J. M.; Becke, A. D. *Chem. Phys. Lett.* **1995**, *233*, 134.
(43) van Mourik, T. *Chem. Phys.* **2004**, *304*, 317.
(44) Wodrich, M. D.; Corminboeuf, C.; Schleyer, P. V. *Org. Lett.* **2006**, *8*, 3631.
(45) Dunning, T. H. *J. Chem. Phys.* **1989**, *90*, 1007.
(46) Kendall, R. A.; Dunning, T. H.; Harrison, R. J. *J. Chem. Phys.* **1992**, *96*, 6796.
(47) Peterson, K. A.; Dunning, T. H. *J. Chem. Phys.* **2002**, *117*, 10548.
(48) Woon, D. E.; Dunning, T. H. *J. Chem. Phys.* **1993**, *98*, 1358.
(49) Woon, D. E.; Dunning, T. H. *J. Chem. Phys.* **1994**, *100*, 2975.
(50) Woon, D. E.; Dunning, T. H. *J. Chem. Phys.* **1995**, *103*, 4572.
(51) Pillsbury, N. R.; Zwier, T. S. In preparation, 2008.

JP806691W